

Article

Electromagnetic Shielding Effectiveness and Conductivity of PTFE/Ag/MWCNT Conductive Fabrics Using the Screen Printing Method

Hung-Chuan Cheng ¹ , Chong-Rong Chen ², Shan-hui Hsu ^{1,*} and Kuo-Bing Cheng ^{2,3,*}

¹ Institute of Polymer Science and Engineering, National Taiwan University, Taipei 106, Taiwan; d02549012@ntu.edu.tw

² Department of Fiber and Composite Material, Feng Chia University, Taichung 407, Taiwan; zx25610548as@gmail.com

³ Textile and Material Industrial Research Center, Feng Chia University, Taichung 407, Taiwan

* Correspondence: shhsu@ntu.edu.tw (S.-h.H.); kbcheng@fcu.edu.tw (K.-B.C.)

Received: 23 June 2020; Accepted: 20 July 2020; Published: 22 July 2020



Abstract: The management of the electromagnetic interference (EMI) of thin, light, and inexpensive materials is important for consumer electronics and human health. This paper describes the development of conductive films that contain a silver (Ag) flake powder and multiwall carbon nanotube (MWCNT) hybrid grid on a polytetrafluoroethylene (PTFE) film for applications that require electromagnetic shielding (EMS) and a conductive film. The Ag and MWCNT hybrid grid was constructed with a wire diameter and spacing of 0.5 mm. The results indicated that the proposed conductive films with 0.4 wt% MWCNTs had higher electromagnetic shielding effectiveness (EMSE) and electrical conductivity than those with other MWCNT loading amounts. The results also showed that the film with 0.4 wt% MWCNT loading had a high 62.4 dB EMSE in the 1800 MHz frequency and 1.81×10^4 S/cm electrical conductivity. This combination improved stretchability, with 10% elongation at a 29% resistivity change rate. Conductive films with Ag/MWCNT electronic printing or lamination technologies could be used for EMI shielding and electrically conductive applications.

Keywords: Ag/MWCNT; EMSE; laminated woven fabric; PTFE film; screen printing

1. Introduction

Traditional materials that can be used for electromagnetic shielding are metal, ceramic, and plastic materials. During low-frequency magnetic field shielding, absorption loss is more important than reflection loss, so steel, plastic materials, or high-permeability magnetic materials are generally used; during high-frequency magnetic field shielding, reflection loss is rather critical, thus, aluminum foil or conductive coating materials are selected [1]. With the advent of the 5th generation (5G) mobile network, self-driving cars, cloud computing, and various electronic products are accelerating the promotion of various specifications of the wireless network. The number of small-cell base stations for the 5G millimeter-wave is expected to be 60 times that of traditional 4G stations. In addition, the large number of sensing elements used in self-driving systems means that people will be exposed to GHz UHF (ultrahigh frequency) transmission; thus, the issue of the impact of electromagnetic waves on human health will come to the fore [2,3]. Additionally, the high transmission efficacy and large number of high-power components that are used in radio frequency (RF) antenna modules and base station basic circuits, e.g., integrated circuits (ICs), system on a chips (SoCs), system in packages (SiPs), antenna in packages (AiPs), power amplifiers, switches, and passive components, cause substantial heat problems. The construction of a healthy indoor environment in modern buildings that is comfortable, convenient, and safe, for example, is the topic of discussion herein. In general,

as long as the electrical equipment is properly grounded and the transformer equipment is shielded by electromagnetic shields in new residential projects, the harm from low-frequency electric fields can be greatly reduced. However, old houses are not grounded, and the source of the electromagnetic waves is outdoors or cannot be solved with high-frequency and ultrahigh frequency electromagnetic radiation; thus, this situation presents a risk to human health.

In the application of EMI shielding films, the conductivity and flexibility of conductive materials are directly related to EMSE and reliability. The migration process of electrons is a key factor affecting the overall electrical properties of conductive composites. There are generally three well-known mechanisms of electrical conductivity in composite materials: percolation, tunneling, and field emission. Percolation theory describes the conductive behavior when the proportion of conductive filler reaches a certain content, and the filler materials are in close contact or the gap is less than 1 nm. The tunneling effect occurs when the applied voltage is low and the distance between the filler materials is less than 10 nm; even if there is no direct contact between the filler materials, electrons can still pass through the gap to achieve conduction. The field emission effect occurs when the filler content is low, but the application of a high electric field can cause the migration of electrons through the isolation layer [4–6].

Based on the price factor and the component requirement, silver paste is the most used in the application of traditional thick film products (e.g., printed circuit boards, membrane switches, passive component electrodes, photovoltaics, radio frequency identification (RFID) devices, and sensors). The addition of multiwall carbon nanotubes (MWCNTs) can increase the probability of conductive fillers contacting each other and can prevent conductivity from decreasing when the distance between the conductive fillers is greater than 10 nm. In addition, a small amount of MWCNTs can increase electrical conductivity, thermal conductivity, and mechanical strength [7–10]. The addition of MWCNTs has a cost advantage over simply adding conductive fillers.

This research provides a method to improve high-frequency electromagnetic shielding and thermal properties [11]. By introducing MWCNTs to increase the conductivity and stretchability of conductive silver paste, screen printing can be used to print an effective shielding circuit [12–15]. A polytetrafluoroethylene (PTFE) substrate can be attached to the nonwoven EMI shielding film with a low manufacturing cost, high EMSE, and high reliability [16–19]. Compared with the weight and thickness of steel, ceramic materials, and plastic materials, the samples made in this experiment can be easily applied to curtains, microwave ovens, or electronic equipment to cover woven fabrics, substation shielding films, smart textile wearable products, and protective clothing, for example.

2. Experimental Details

2.1. Preparation of Ag/MWCNT Hybrid Conductive Paste

A well-dispersion of 4 wt% MWCNT was prepared by combining a specific weight of gum arabic (GA, 0.14 g), poly(acrylic acid sodium salt) (PAAS, 0.06 g), isopropyl alcohol (IPA, 9.6 g), and MWCNTs (0.4 g) in ultrasonic and planetary centrifugal mixers (Figure 1) [20,21].

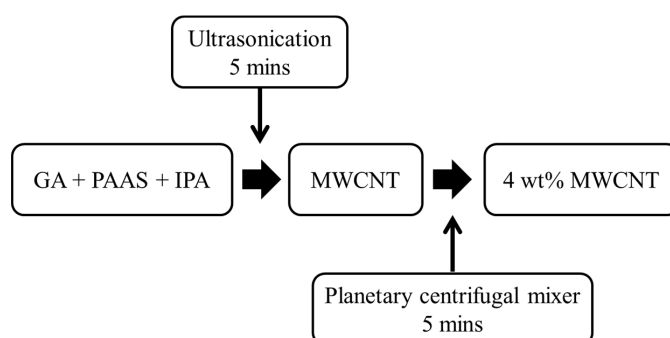


Figure 1. The preparation process of 4 wt% multiwall carbon nanotube (MWCNT) dispersion.

Ten grams of conductive Ag/MWCNT composite paste were used for the preparation and formulation processes shown in Figure 2 and Table 1. Appropriate amounts of silver paste and 4 wt% MWCNT dispersion, with weights (g) of 9.98:0.35, 9.97:0.5, 9.96:0.68, 9.95:0.85, and 9.94:1.03, respectively, were formulated. The concentrations of MWCNT of 0.2, 0.3, 0.4, 0.5, and 0.6 wt% in the Ag/MWCNT composite paste were prepared by a planetary centrifugal mixer for 2 minutes. The referenced codes refer to the different MWCNT contents, such as 4SC indicating a solid content of MWCNT (SCM) that accounts for 0.4 wt% of the solid content of silver paste (SCSP).

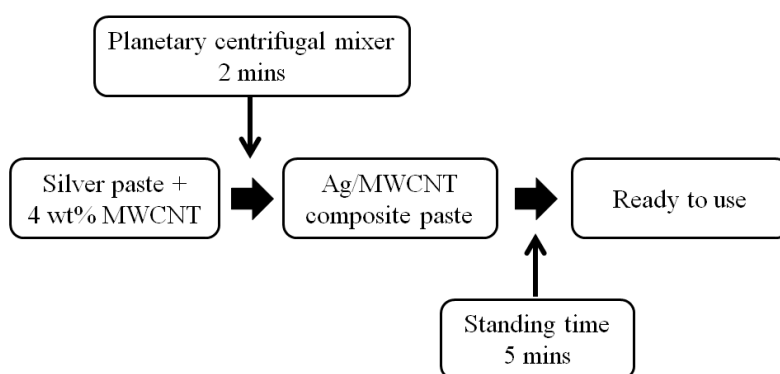


Figure 2. The preparation process of Ag/MWCNT pastes.

Table 1. The compositions of Ag/MWCNT hybrid conductive pastes.

	Silver Paste (g)	*1 SCSP (wt%)	MWCNT Dispersion (g)	*2 SCM (wt%)	SCM/SCSP (wt%)
Reference	10	6.8	-	-	-
2SC	9.98	6.786	0.35	0.014	0.2
3SC	9.97	6.78	0.5	0.02	0.3
4SC	9.96	6.773	0.68	0.027	0.4
5SC	9.95	6.766	0.85	0.034	0.5
6SC	9.94	6.759	1.03	0.041	0.6

*1 Solid Content of Silver Paste (SCSP). *2 Solid Content of MWCNT (SCM).

The quality of raw materials is very important when we do formula modification. It needs to balance the compatibility, electrical properties, and rheology for screen printing of the materials. Thus, measurements of 2.5 to 20 μm for the particle size of the silver flake, $58\pm 2\%$ for silver solid content, and 23,000 cps for viscosity can approach the highest electrical conductivity and good bending ability of the conductive silver paste (AG-1003, HongChen Materials Corporation, Taiwan). The average diameter of the MWCNTs was 8 to 15 nm, the length was 10 to 70 μm , the density was 0.1 to 0.15 g/cm^3 , and the surface area was 235 to 275 m^2/g (CP1002M, LG Chemical, Korea) (Figure 3).

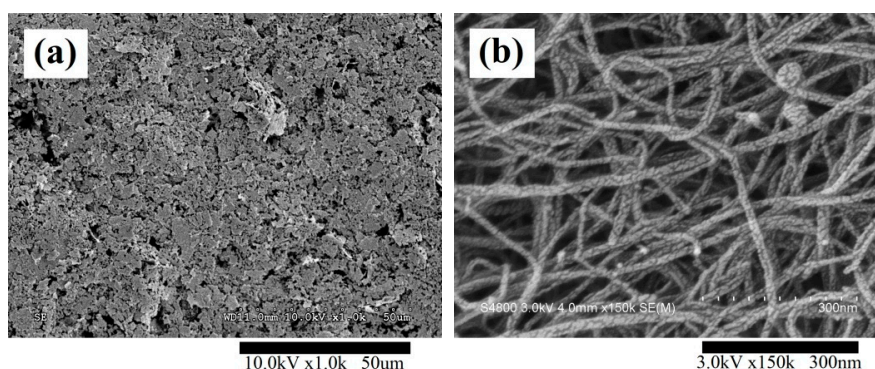


Figure 3. Variable vacuum scanning electron microscopy (VVSEM) image of the (a) conductive silver paste and (b) MWCNT.

2.2. Production of Conductive Laminated Fabrics

A screen printing method was used to fabricate conductive laminated fabrics for this paper. A viscous and conductive composite paste that contained a suitable amount of silver flakes and MWCNTs, thermal plastic urethanes, a multi-solvent system, and additive agents was used during fabrication. The Ag/MWCNT composite paste was fed onto a 300-mesh screen and manipulated with a squeegee to form a grid pattern, in order to save on the material's cost. The grid pattern was constructed with a wire diameter and spacing of 0.5 mm. The recovery area was about 75% of the PTFE film, and thus provided a cost-efficient solution. Adding a certain amount of MWCNTs and making a composite paste with conductive silver paste provided the substantial benefits of reducing raw material cost and improving conductivity.

The PTFE/Ag/MWCNT composite film was laminated to the cotton woven fabric, where polyurethane reactive glue (PUR Glue) was the adhesive layer, with 120 ends/2.54 cm and 80 picks/2.54 cm warp and weft densities, respectively (Figure 4). The warp and weft yarn count was 59.1 tex. The tested specimens used in this investigation are shown in Figure 4. The specimens had a nominal width and length of 15 cm. An Ag/MWCNT conductive circuit was shown on the PTFE substrate, then the printed side of the conductive circuit was laminated onto the woven fabric with PUR glue, then the release paper was removed.

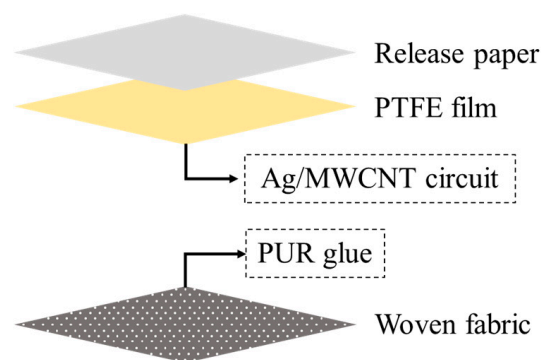


Figure 4. The structure of the laminated fabric (size: 15*15 cm).

2.3. Surface Resistivity, Volume Resistivity and Electrical Conductivity Measurements

Measurements were made using a Loresta-GP MCP-T600 resistivity meter (Mitsubishi Chemical Corporation, Japan), followed by a JIS K 7194 [22]. In order to confirm the stability of the Ag/MWCNT composite paste and screen printing process, volume resistivity (ρ_v) was checked for 3 to 10 samples, and the results show a window within 5% [23].

The stretchability testing was conducted according to ASTM D638 [24], and the proposed bending testing methods reproduced the state of cyclic unloading conditions for 180 degrees by placing the samples between two parallel plates to observe the resistance of the coefficient of variation [25].

2.4. Morphology of PTFE/Ag/MWCNT Conductive Composite Film

The morphology of the conductive circuit was observed using high-resolution variable vacuum scanning electron microscopy (HR-VVSEM).

2.5. Measurement of the Laminated Fabric of PTFE/Ag/MWCNT Conductive Composite Film

The EMSE of the PTFE/Ag/MWCNT conductive composite films was measured by an Elgal set 19A coaxial holder system (EM-21078, ShangHai YinXu Mechanical and Electrical Equipment Co., Ltd., China) [26,27]. The thermal conductivity (mW/m.K) and thermal diffusivity (mm^2/S) were measured by a thermal property analyzer (Alambeta, Sensor Instruments & Consulting REG.

NR., Czech Republic) [28]. An infrared thermal imaging camera (FLIR-A320, FLIR Systems Inc., USA) was used to observe the temperature difference of the PTFE/Ag/MWCNT conductive composite film [29].

3. Results and Discussion

3.1. Morphological Analysis of PTFE/Ag/MWCNT Composite Film

In this study, the quality of the Ag/MWCNT composite paste and the morphology of the circuit are very important due to the correlation of conductivity, skin effect, and EMSE. The electric current flows mainly along the skin of the conductor and does not penetrate to the core. The skin depth decreases as the radio frequency increases, so the surface roughness of the circuit is one of the major parameters that needs to be checked when high incident frequency applications are used. The SEM images of the Ag/MWCNT conductive circuit in sample 4SC are shown in Figure 5a. However, it is difficult to produce hand-made samples with high uniformity (Figure 5b), resulting in defects in the circuit and poor EMSE. Figure 5c,d show that MWCNTs can provide a complete conductive network to improve electrical conductivity.

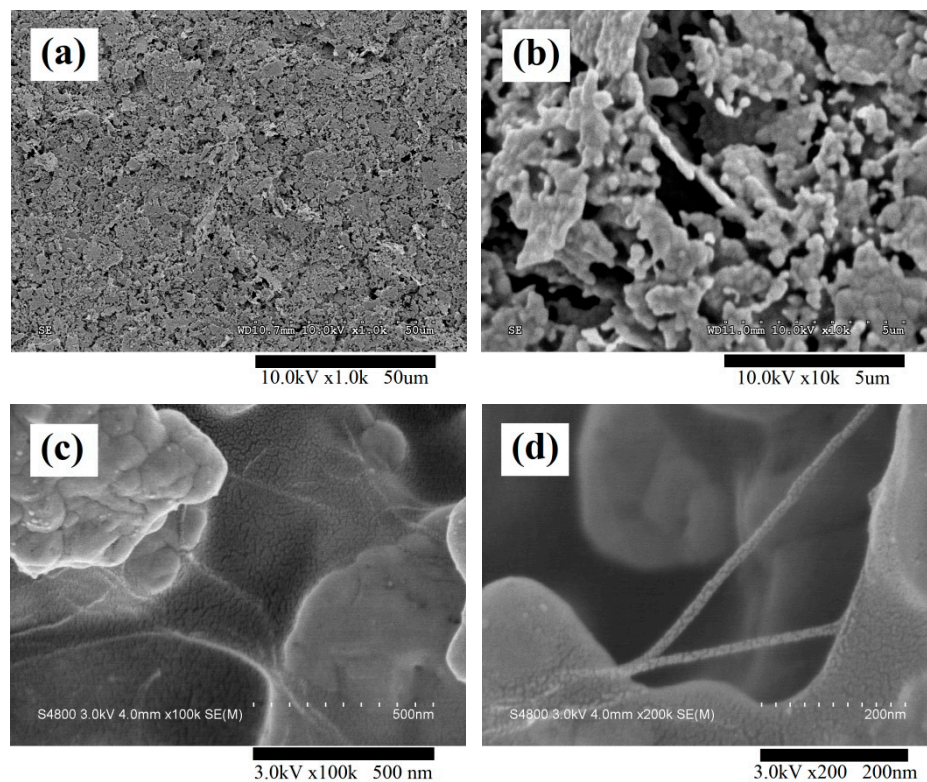


Figure 5. VVSEM images of the Ag/MWCNT conductive circuit in sample 4SC. (a) Topography, (b) morphology and arrangement of the silver flakes, (c,d) connections between the MWCNTs and silver flakes.

A conductive PTFE/Ag/MWCNT composite film was produced with a thermal curable Ag/MWCNT composite conductive paste and a PTFE substrate. A good connection of the conductivity of Ag/MWCNT fillers, a specified grid pattern, and a PTFE substrate improved the electrical properties, flexibility, and feel of the fabric, and saved on the material's consumption. Since the surface roughness of PTFE substrate is smaller than fabric, it can ameliorate the grid pattern of the printed situation to get better and more stable electrical conductivity, flexibility, and EMSE. Through changing the recipe of the Ag/MWCNT composite paste, the rheology was changed. The optical microscope (OM) image of Figure 6b (4SC) shows better printing quality than Figure 6a (pure silver). This result demonstrates that higher viscosity was more suitable for the hand-made screen printing process.

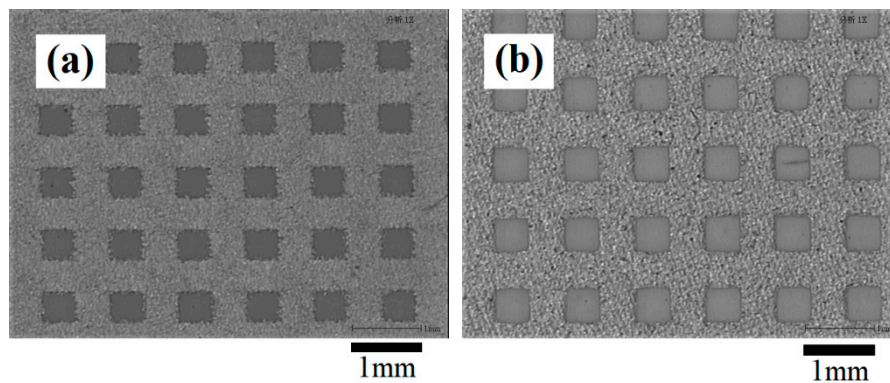


Figure 6. Optical microscope (OM) image of the grid pattern of (a) pure conductive silver paste and (b) 4SC.

3.2. Electrical and Mechanical Properties of PTFE/Ag/MWCNT Composite Film

Figure 7a shows the variation in the conductivity of the PTFE/Ag/MWCNT composite films when changing the amount of MWCNTs added to the conductive Ag/MWCNT composite paste. To produce much smoother mesh wires, dibasic esters (DBE) can be a thinner to adjust the rheology of the Ag/MWCNT conductive paste, which makes the process of screen printing easier, and optimal electrical conductivity was obtained with 0.4 wt% MWCNT loading (4SC). For the composite film, electrical conductivity reached 1.81×10^4 S/cm, with the 6SC film having the lowest conductivity. The maximum conductivity of the 4SC composite film is 30% higher than the conductivity of the 6SC film. The conductivity trends of PTFE/Ag/MWCNT films demonstrated that loading MWCNTs did not do much good. This can be explained by percolation theory. MWCNT loading had a notable influence on the electrical properties of the films. Thus, conductivity can be modified through different component ratios of silver powder and MWCNTs (by varying the concentration, uniformity of the conductive network, or Ag/MWCNT wire density). Figure 7b shows the results in the surface resistivity of the PTFE/Ag/MWCNT conductive films as a function of the amount of MWCNTs added to the conductive Ag/MWCNT composite paste. The optimal surface resistivity also occurred with a loading of 0.4 wt% MWCNT (4SC), whereas the 6SC film had the highest surface resistivity.

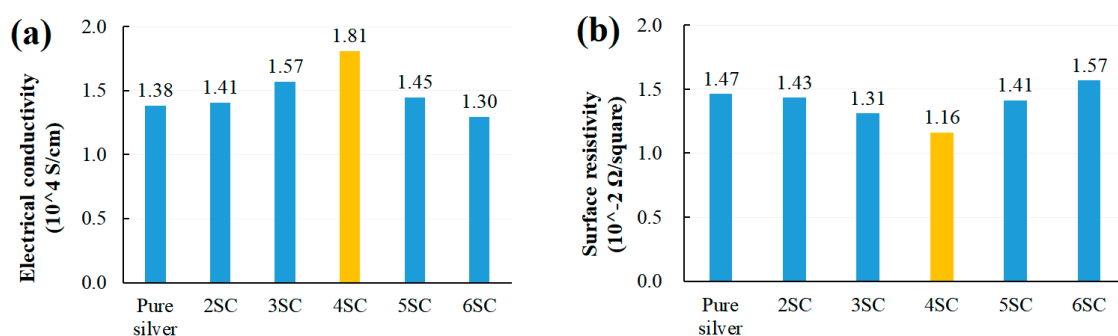


Figure 7. Variation in the (a) conductivity (Siemens/cm) and (b) surface resistivity of the conductive PTFE/Ag/MWCNT films.

When electronic products, such as flexible substrates, are used, the products undergo a certain degree of bending and deformation, causing circuit damage that impacts electrical conductivity. In textile products, it is necessary to consider the damage caused by multiple cleanings and laundry. At present, an increasing number of substrates are malleable. Therefore, conductive materials that can withstand tensile and bending resistance are becoming important. The effects of tensile elongation and hybrid paste formulation on the changing percentage of electrical resistance of the PTFE/Ag/MWCNT

conductive films are shown in Figure 8a. The PTFE/Ag/MWCNT conductive films had an improved variation in electrical resistance under 10% tensile elongation. The improvement in flexibility can be seen in the stretchability and cyclic bending test results. Through the coefficient of variation, it can be observed that under 10% elongation conditions, 3SC (16.7%) and 4SC (15.1%) showed increased stability (Figure 8b). Similar results can be seen in the cyclic bending test (0% for 4SC and 5SC) (Figure 9). It can be seen from the cyclic bending test that there was an increase in the number of cyclic bending cycles of the composite film. The change in resistivity was extremely small because MWCNTs are very strong, their mechanical strength is very good, and it is not easy to break the composite film after cyclic bending. Under 1000 cycles of the bending test, the coefficient of variation did not change for 4SC and 5SC, which showed excellent reproducibility, reliability, and stability (Figure 9). The high-aspect-ratio MWCNTs contributed to the multiple conductive pathways, tough mechanical properties, flexibility, and strength of the Ag/MWCNT composite paste under testing.

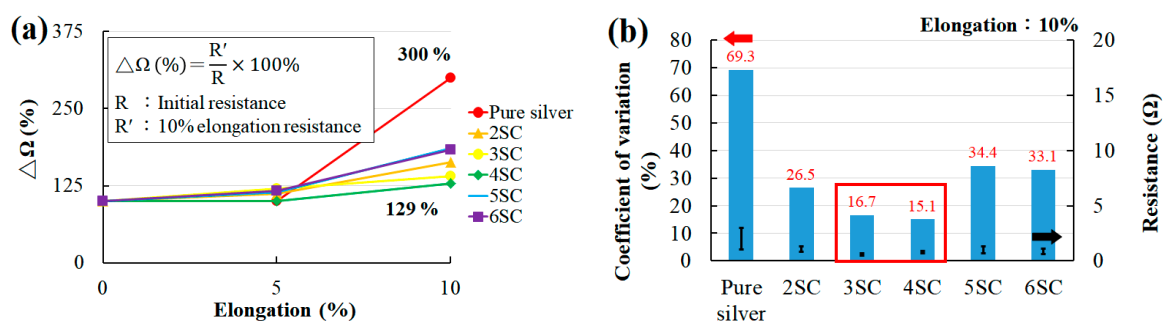


Figure 8. (a) The effects of tensile elongation and hybrid paste formulation on the changing percentage of the electrical resistance of PTFE/Ag/MWCNT conductive films and (b) the coefficient variance of the electrical resistance of PTFE/Ag/MWCNT film under 10% tensile elongation.

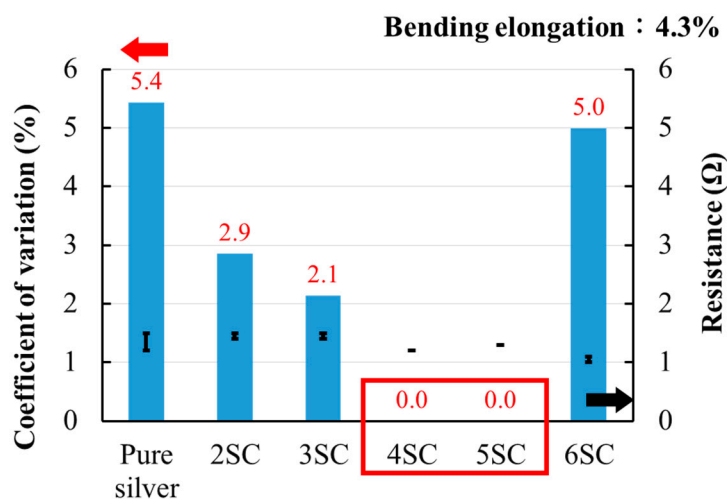


Figure 9. CV% of the electrical resistance of the PTFE/Ag/MWCNT conductive films under 1000 cycles of bending testing.

3.3. EMSE Analysis of PTFE/Ag/MWCNT Conductive Laminated Fabrics

The EMSE results (measurement frequency is 5 MHz to 3000 MHz) of the conductive laminated fabrics are presented in Figure 10 and Table 2. A regular up and down pattern with frequencies from 5 MHz to 3000 MHz is shown. The PTFE/Ag/MWCNT conductive films with an addition of 0.4 wt% MWCNTs displayed the highest EMSE, compared to the other PTFE/Ag/MWCNT films. According to the electromagnetic wave shielding test, the PTFE/Ag/MWCNT conductive laminated fabric printed with the Ag/MWCNT composite paste had a good electromagnetic wave shielding effect, and its EMSE

value exceeded 40 dB. At a frequency of 300 MHz (domestic wireless telephone), the 3SC has a good EMSE value of 50.1 dB; at a frequency of 1800 MHz (4G mobile phone), 4SC has the best EMSE value of 62.4 dB; at a frequency of 2450 MHz (microwave oven), 4SC has the best EMSE of 59.9 dB. The results reach very good to excellent levels, according to the classifications of EMSE for general purposes (Table 3).

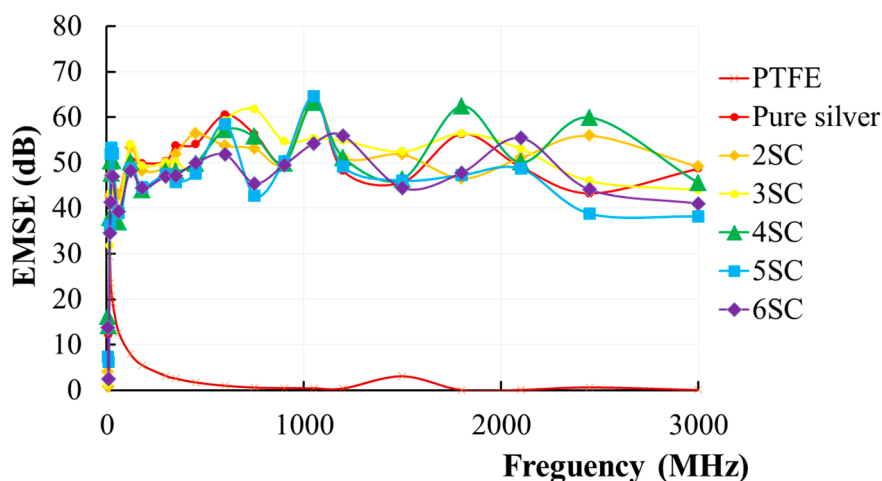


Figure 10. EMSE vs. frequency plots for different MWCNT contents in the PTFE/Ag/MWCNT conductive laminated fabrics.

Table 2. EMSE data for the applications of 300 MHz, 1800 MHz, and 2450 MHz.

Application/Unit: dB	PTFE	Pure silver	2SC	3SC	4SC	5SC	6SC
300 MHz (Cordless telephone)	3.1	50.3	48.9	50.1	48.0	47.5	47.1
1800 MHz (4G mobile phone)	0.1	56.3	46.5	56.4	62.4	47.3	47.8
2450 MHz (Microwave oven)	0.6	43.3	55.9	46	59.9	38.8	44.1

Table 3. The classifications of EMSE for general purposes.

Type	Class 5 Excellent	Class 4 Very Good	Class 3 Good	Class 2 Moderate	Class 2 Fair
EMSE ranges	SE > 60	60 ≥ SE > 50	50 ≥ SE > 40	40 ≥ SE > 30	30 ≥ SE > 20

3.4. Thermal Analysis of PTFE/Ag/MWCNT Conductive Laminated Fabrics

Table 4 shows the thermal properties of PTFE/Ag/MWCNT conductive laminated fabric. It can be seen from the thermal property tests that with an increase in the amount of MWCNTs, the thermal conductivity of the laminated fabric tended to rise first and then decrease because the addition of the MWCNTs correspondingly reduced the silver solid content, resulting in a downward trend. Sample 4SC showed the highest thermal conductivity coefficient and thermal diffusion values of 37.1 mW/m.K and 0.240 mm²/s, respectively. This is probably because the 4SC tested sample had the best thermal conductive network. However, as the MWCNT amount increased, agglomeration increased.

Figure 11 and Table 5 present the results in the temperature difference of the conductive laminated fabrics for the different formulations. The temperature difference of the laminated fabric increased first and then decreased because the addition of MWCNTs correspondingly reduced the silver solid content, resulting in a downward trend. From the far infrared thermal imaging test, it can be seen that the laminated fabric with the added MWCNTs had a better heating effect than the fabric that did not

contain the MWCNTs because the MWCNTs have high thermal conductivity and good heat transfer characteristics. The 4SC has the highest temperature increase of 5.6 °C and temperature decrease of 4.0 °C.

Table 4. Thermal properties of PTFE/Ag/MWCNT conductive laminated fabrics.

Sample/Data	Pure Silver	2SC	3SC	4SC	5SC	6SC
Thermal conductivity (mW/m.K)	35.5	36.3	36.7	37.1	36.5	36.2
Thermal diffusivity (mm ² /s)	0.132	0.157	0.217	0.240	0.200	0.118

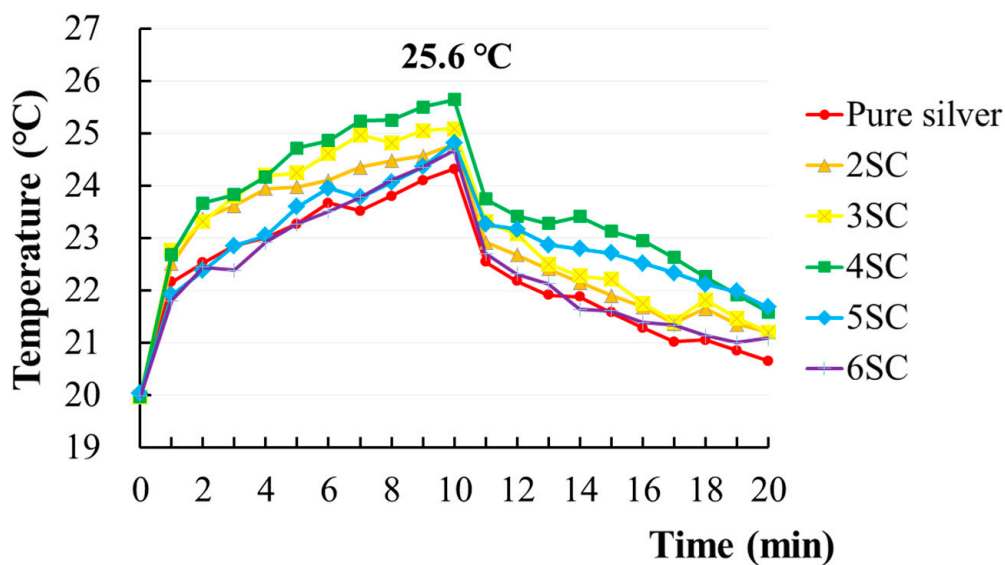


Figure 11. Temperature changes under far infrared irradiation of PTFE/Ag/MWCNT conductive laminated fabrics.

Table 5. Temperature changes during far-infrared irradiation of PTFE/Ag/MWCNT conductive laminated fabrics.

Sample	T0	T10	T20	$\Delta T1$ (T10-T0)	$\Delta T2$ (T10-T20)	$\Delta T3$ (T20-T0)
Pure silver	20.0	24.3	20.7	4.3	3.6	0.7
2SC	20.0	24.8	21.2	4.8	3.6	1.2
3SC	20.0	25.1	21.2	5.1	3.9	1.2
4SC	20.0	25.6	21.6	5.6	4.0	1.6
5SC	20.0	24.8	21.7	4.8	3.1	1.7
6SC	20.0	24.7	21.1	4.7	3.6	1.1

4. Conclusions

In this paper, an Ag/MWCNT composite conductive paste was applied to a PTFE film, using a screen printing method to produce a grid pattern with high electrical conductivity, EMSE, thermal conductivity, and diffusivity functions. This PTFE/Ag/MWCNT composite film was then used to laminate woven fabric, providing a low cost material with highly stable electrical properties for printing, high durability, good softness, high EMSE, and improved thermal properties. The EMSE of the PTFE/Ag/MWCNT conductive laminated woven fabrics can be adjusted via designing different grid patterns and controlling the ratio of Ag/MWCNT. It can be observed that PTFE/Ag/MWCNT conductive laminated fabrics may

have applications as home textiles which solve health and electrical issues related to electromagnetic shielding and thermal problems, being especially easy to use because of their flexibility. The 4SC conductive fabric sample had a higher EMSE than other specimens for almost all frequency ranges from 120 to 3000 MHz. The EMSE and thermal properties of the PTFE/Ag/MWCNT laminated fabrics showed improved performance and are suitable for use in domestic electronic appliances and household textiles. Since MWCNT shows excellent improvement of flexibility and elongation, it has the potential to acquire the stretchable property of conductive ink in the future.

Author Contributions: Conceptualization, H.-C.C.; methodology, H.-C.C.; validation, H.-C.C. and C.-R.C.; formal analysis, C.-R.C.; investigation, C.-R.C.; resources, H.-C.C. and K.-B.C.; data curation, C.-R.C.; writing—original draft preparation, H.-C.C.; writing—review and editing, S.-h.H. and K.-B.C.; visualization, C.-R.C. and H.-C.C.; supervision, S.-h.H. and K.-B.C.; project administration, K.-B.C.; funding acquisition, K.-B.C. All authors have read and agreed to the published version of the manuscript.

Funding: This research was funded by the Ministry of Science and Technology (MOST) of Taiwan to Feng Chia University under MOST-108-2218-E-035-001.

Acknowledgments: This work was supported by the Ministry of Science and Technology (MOST) of Taiwan to Feng Chia University under MOST-108-2218-E-035-001. The authors also thank the Institute of Polymer Science and Engineering, National Taiwan University, Taiwan, for guidance on materials and formulation principles, and the Fiber Structure Lab of Feng Chia University, Taiwan, for providing all necessary instruments.

Conflicts of Interest: The authors declare no conflicts of interest.

References

1. Shukla, V. Review of electromagnetic interference shielding materials fabricated by iron ingredients. *Nanoscale Adv.* **2019**, *1*, 1640–1671. [[CrossRef](#)]
2. Al-Falahy, N.; Alani, O.Y. Technologies for 5G Networks: Challenges and Opportunities. *IT Prof.* **2017**, *19*, 12–20. [[CrossRef](#)]
3. Zhao, K.; Ying, Z.; He, S. EMF Exposure Study Concerning mmWave Phased Array in Mobile Devices for 5G Communication. *IEEE Antennas Wirel. Propag. Lett.* **2016**, *15*, 1132–1135. [[CrossRef](#)]
4. He, L.-X.; Tjong, S.-C. Internal field emission and conductivity relaxation in carbon nanofiber filled polymer system. *Synth. Met.* **2010**, *160*, 2085–2088. [[CrossRef](#)]
5. Hashemi, R.; Weng, G.J. A theoretical treatment of graphene nanocomposites with percolation threshold, tunneling-assisted conductivity and microcapacitor effect in AC and DC electrical settings. *Carbon* **2016**, *96*, 474–490. [[CrossRef](#)]
6. Bilotti, E.; Zhang, H.; Deng, H.; Zhang, R.; Fu, Q.; Peijs, T. Controlling the dynamic percolation of carbon nanotube based conductive polymer composites by addition of secondary nanofillers: The effect on electrical conductivity and tuneable sensing behavior. *Compos. Sci. Technol.* **2013**, *74*, 85–90. [[CrossRef](#)]
7. Chun, K.-Y.; Oh, Y.; Rho, J.; Ahn, J.-H.; Kim, Y.-J.; Choi, H.R.; Naik, S. Highly conductive, printable and stretchable composite films of carbon nanotubes and silver. *Nat. Nanotechnol.* **2010**, *28*, 853–857. [[CrossRef](#)]
8. Maiti, S.; Suin, S.; Shrivastava, N.K.; Khatua, B.B. A strategy to achieve high electromagnetic interference shielding and ultra low percolation in multiwall carbon nanotube-polycarbonate composites through selective localization of carbon nanotubes. *RSC Adv.* **2014**, *4*, 7979–7990. [[CrossRef](#)]
9. Rosca, I.D.; Hoa, S.V. Highly conductive multiwall carbon nanotube and epoxy composites produced by three-roll milling. *Carbon* **2009**, *47*, 1958–1968. [[CrossRef](#)]
10. Ma, R.; Kwon, S.; Zheng, Q.; Kwon, H.Y.; Kim, J.I.; Choi, H.R.; Baik, S. Carbon-Nanotube/Silver Networks in Nitrile Butadiene Rubber for Highly Conductive Flexible Adhesives. *Adv. Mater.* **2012**, *24*, 3344–3349. [[CrossRef](#)]
11. Pawar, S.P.; Biswas, S.; Kar, G.P.; Bose, S. High frequency millimetre wave absorbers derived from polymeric nanocomposites. *Polymer* **2016**, *84*, 398–419. [[CrossRef](#)]
12. Hassan, M.; Afify, A.S.; Ataalla, M.; Milanese, D.; Tulliani, J.-M. New ZnO-Based Glass Ceramic Sensor for H₂ and NO₂ Detection. *Sensors* **2017**, *17*, 2538. [[CrossRef](#)] [[PubMed](#)]
13. Afify, A.S.; Ahmad, S.; Khushnood, R.A.; Jagdale, P.; Tulliani, J.-M. Elaboration and characterization of novel humidity sensor based on micro-carbonized bamboo particles. *Sens. Actuators B Chem.* **2017**, *239*, 1251–1256. [[CrossRef](#)]

14. Erath, D.; Filipović, A.; Retzlaff, M.; Goetz, A.K.; Clement, F.; Biro, D.; Preu, R. Advanced screen printing technique for high definition front side metallization of crystalline silicon solar cells. *Sol. Energy Mater. Sol. Cells* **2010**, *94*, 57–61. [[CrossRef](#)]
15. Hsu, C.-P.; Guo, R.-H.; Hua, C.-C.; Shih, C.-L.; Chen, W.-T.; Chang, T.-I. Effect of polymer binders in screen printing technique of silver pastes. *J. Polym. Res.* **2013**, *20*, 277. [[CrossRef](#)]
16. Kolanowska, A.; Janas, D.; Herman, A.P.; Jędrzyński, R.G.; Giżewski, T.; Boncel, S. From blackness to invisibility—Carbon nanotubes role in the attenuation of and shielding from radio waves for stealth technology. *Carbon* **2018**, *126*, 31–52. [[CrossRef](#)]
17. Kim, Y.J.; An, K.J.; Suh, K.S.; Choi, H.-D.; Kwon, J.H.; Chung, Y.-C.; Kim, W.N.; Lee, A.-K.; Choi, J.-I.; Yoon, H.G. Hybridization of oxidized MWNT and silver powder in polyurethane matrix for electromagnetic interference shielding application. *IEEE Trans. Electromagn. Compat.* **2005**, *47*, 872–879. [[CrossRef](#)]
18. Shajari, S.; Arjmand, M.; Pawar, S.P.; Sundararaj, U.; Sudak, L.J. Synergistic effect of hybrid stainless steel fiber and carbon nanotube on mechanical properties and electromagnetic interference shielding of polypropylene nanocomposites. *Compos. Part B* **2019**, *165*, 662–670. [[CrossRef](#)]
19. Kwon, S.; Ma, R.; Kim, U.; Choi, H.R.; Baik, S. Flexible electromagnetic interference shields made of silver flakes, carbon nanotubes and nitrile butadiene rubber. *Carbon* **2014**, *68*, 118–124. [[CrossRef](#)]
20. Lin, M.; Gai, Y.; Xiao, D.; Tan, H.; Zhao, Y. Preparation of pristine graphene paste for screen printing patterns with high conductivity. *Chem. Phys. Lett.* **2018**, *713*, 98–104. [[CrossRef](#)]
21. Jiang, Y.; Song, H.; Xu, R. Research on the dispersion of carbon nanotubes by ultrasonic oscillation, surfactant and centrifugation respectively and fiscal policies for its industrial development. *Ultrason. Sonochem.* **2018**, *48*, 30–38. [[CrossRef](#)] [[PubMed](#)]
22. Kirkpatrick, S. Percolation and Conduction. *Rev. Mod. Phys.* **1973**, *45*, 574–588. [[CrossRef](#)]
23. Cheng, H.-C.; Chen, C.-R.; Hsu, S.-H.; Cheng, K.-B. The electromagnetic shielding effectiveness of laminated fabrics using electronic printing. *Polym. Compos.* **2020**, *41*, 2568–2577. [[CrossRef](#)]
24. Choi, J.H.; Lee, K.Y.; Kim, S.W. Ultra-bendable and durable Graphene—Urethane composite/silver nanowire film for flexible transparent electrodes and electromagnetic-interference shielding. *Compos. Part B Eng.* **2019**, *177*, 107406. [[CrossRef](#)]
25. Leterrier, Y. 1-Mechanics of curvature and strain in flexible organic electronic devices. In *Handbook of Flexible Organic Electronics: Materials Manufacturing and Applications*; Woodhead Publishing: Oxford, UK, 2015; Volume 3, pp. 3–36.
26. Hewlett-Packard Co. *HP 8752 Operation Manual, Performance Tests*; Hewlett-Packard Co.: Palo Alto, CA, USA, 1996; Volume 4.
27. Cheng, K.-B.; Ramakrishna, S.; Ueng, T.H.; Lee, M.L. Electromagnetic Shielding Effectiveness of the Stainless Steel/Polyester Woven Fabrics. *Text. Res. J.* **2001**, *71*, 42–49. [[CrossRef](#)]
28. Hes, L.; Araujo, M.D.; Djulay, V.V. Effect of Mutual Bonding of Textile Layers on Thermal Insulation and Thermal Contact Properties of Fabric Assemblies. *Text. Res. J.* **1996**, *66*, 245–250. [[CrossRef](#)]
29. Banerjee, D.; Chattopadhyay, S.K.; Tuli, S. Infrared thermography in material research—A review of textile applications. *Indian J. Fibre Text. Res.* **2013**, *38*, 427–437.



© 2020 by the authors. Licensee MDPI, Basel, Switzerland. This article is an open access article distributed under the terms and conditions of the Creative Commons Attribution (CC BY) license (<http://creativecommons.org/licenses/by/4.0/>).